

SUPPLEMENTARY DATA

Table S1

Primer name	Sequence 5' to 3'	Description
Rv8cF-BamHI	GCGGATCCATGAGTGAGCAGGTGGAAAC	Forward for <i>gfp-cwsA_{tb}</i> fusion
Rv8cR-XbaI	TTGCTCTAGATCAGGAGCGCGGTTGCACCT	Reverse for sense <i>cwsA_{tb}</i> overproduction, and <i>gfp</i> fusions
Rv8c-solR-XbaI	TTGCTCTAGATCATTGCTGCGACGTTGGGTCCGG	Reverse for <i>gfp-cwsA_{tb}-soluble part</i> fusion
MVM469	GCGACCAGTACTAAAGGAGAAGAACTTTTCACT	Forward for <i>gfp</i>
Rv8cF-BamHI-B2H	TCTAGA'GGATCC'CATGAGTGAGCAGGTGGAAAC	Forward for <i>cwsA_{tb}</i> for bacterial two hybrid assay
Rv8cR-KpnI-B2H	TTACTTA'GGTACC'CGGGAGCGCGGTTGCACCTCGA	Reverse for <i>cwsA_{tb}</i> for bacterial two hybrid assay
Rv8c-solR-KpnI-B2H	TTACTTA'GGTACC'CGTTTCTGCGACGTTGGGTCC	Reverse for <i>cwsA_{tb}-soluble part</i> for bacterial two hybrid assay
Wag31F-BamHI-B2H	TCTAGA'GGATCC'CATGCCGCTTACACCTGCCGA	Forward for <i>wag31</i> for bacterial two hybrid
Wag31R-KpnI-B2H	TTACTTA'GGTACC'CGGTTTTTGCCCCGGTTGAATTGATCGA	Reverse for <i>wag31</i> for bacterial two hybrid
Rv8cF-KO	AAAA'CTGCAG'CTCGGGGTGGAAGCTC	Forward upstream <i>cwsA_{smeg}</i> for gene knockout
Rv8cR-KO	GGAATTC'CATATG'TTAATTAA'GACGACAGCCCGTTGCCAAC	Reverse downstream <i>cwsA_{smeg}</i> for gene knockout
Rv8cF-PacI	AGAACC'TTAATTAA'GAGCCCCACCAGGGAGGAAGCCGAACGATGAGTGAGCAGGTGGAAAC	Forward for <i>cwsA_{tb}-soluble part</i> in pLR52
Rv8c-solR-SwaI	ATCGG'ATTTAAAT'TCATTGCTGCGACGTTGGGTCCGG	Reverse for <i>cwsA_{tb}-soluble part</i> in pLR52
Msmeg0023F-ClaI	CC'ATCGAT'TGGTTGCCGAACAGTGCAT	Forward for <i>cwsA_{smeg}</i> under native promoter
Msmeg0023F-XbaI	TTGC'TCTAGA'TTCAGGGCTTGGGGGCGACCTC	Reverse for <i>cwsA_{smeg}</i> under native promoter
MR326	AGAGGATCCCATGGCCGCGGGCGGCGGTGCCGG	Forward for <i>wag31</i> C-terminal domain in BACTH vectors
MVM831	TTACTTAGGTACCCGGTTTTTGCCCCGGTTGAATTGATCGA	Reverse for <i>wag31</i> C-terminal domain in BACTH vectors
MVM920	GGGAATTCCATATGCCGCTTACACCTGCCGA	Forward for <i>wag31</i> in <i>wag31-mCherry</i> fusion
MVM921	GCAGTACTAACAACAACCTGCAGATGGTGAGCAAGGGCGAGGA	Forward for <i>mCherry</i>
MVM922	GTAGTCTAGATTACTTGTACAGCTCGTCCATGC	Reverse for <i>mCherry</i>
MVM923	CACAGTACTGTTTTTGCCCCGGTTGAATT	Reverse for <i>wag31</i> in <i>wag31-mCherry</i> fusion
mmsg23_F	CCAGAGCAGATGTCCGATTG	Forward for qRT-PCR of

		<i>cwsA</i>
msemg23_R	GCTTCCTGGATCGTCTCG	Reverse for qRT-PCR of <i>cwsA</i>
sigAsmeg_F	CCCACCGGGAATTCGTAAG	Forward for qRT-PCR of <i>sigA</i>
sigAsmeg_R	TTGCCGGGCTTGCCTT	Reverse for qRT-PCR of <i>sigA</i>

'BOLD LETTERS' indicate restriction sites.

Supplementary Figures and legends

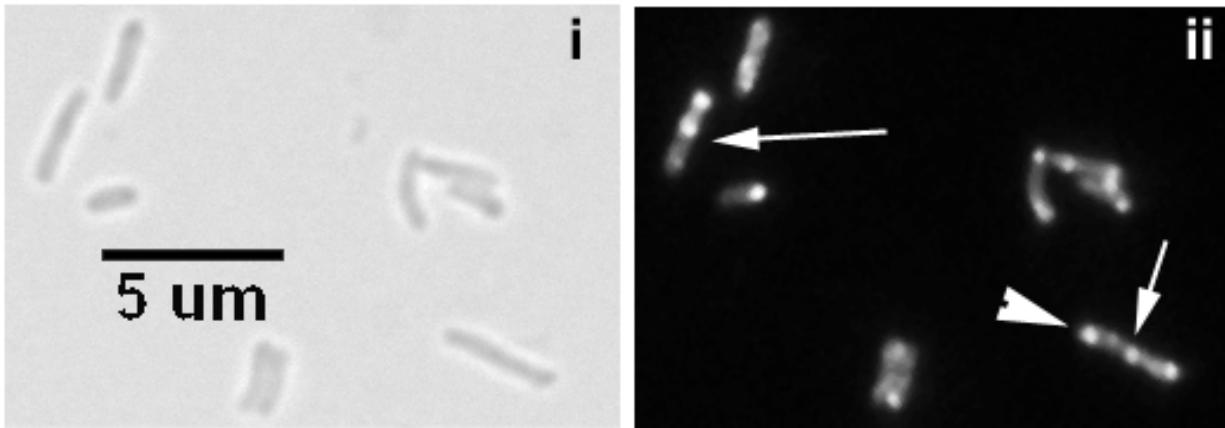


FIG. S1. Localization of *gfp-cwsA* in *M. tuberculosis*. Actively growing cultures of *M. tuberculosis Pami::gfp-cwsA* were induced with 0.2% acetaminde for 48 h, harvested and fixed in 4% paraformaldehyde for 24 h. The cells were examined by bright-field (i) and fluorescence (ii) microscopy as described in the text. Arrow – midcell (new pole) localization; arrowhead – polar localization.

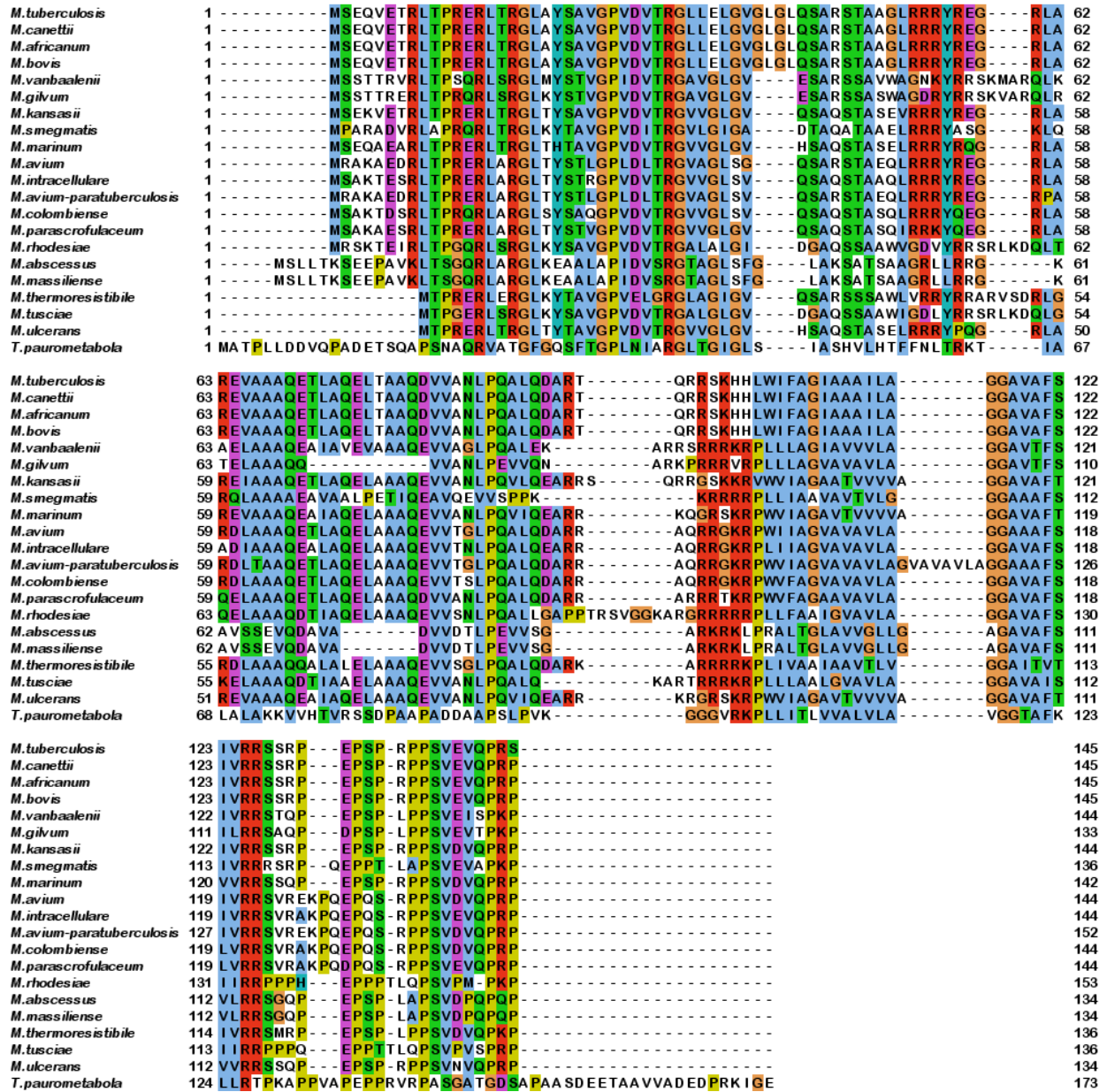


FIG. S2. Amino acid sequence alignment of *cwsA* homologues. CwsA homologs (DUF2562 domain containing) from mycobacterial species and closely related *Tsukamurella paurometabola* were aligned with ClustalX program. The conservation of amino acids with the same properties is indicated with colors, according to ClustalX coloring scheme (<http://www.jalview.org/help/html/colourSchemes/clustal.html>).

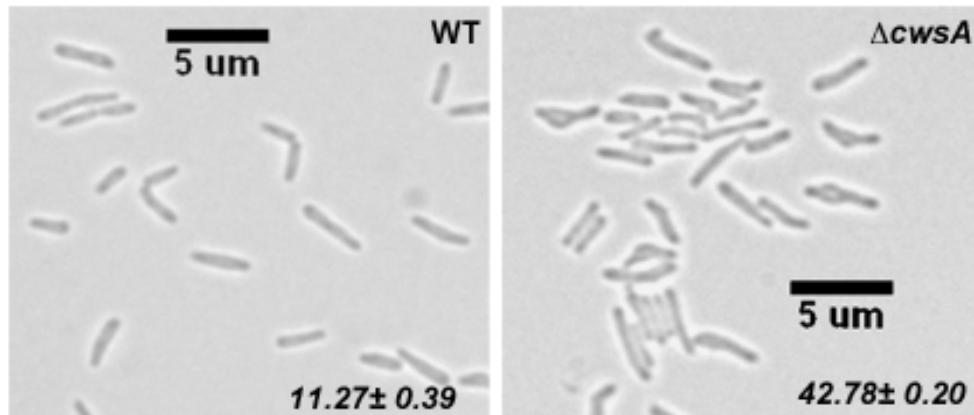


Fig. S3. Morphology of *M. smegmatis* WT and $\Delta cwsA$ stationary phase cultures. Respective strains were grown to $A_{600} \sim 2.0$ and imaged by brightfield microscopy. Data were analyzed and scored for number of bulged (swollen) cells in each strain. Averages \pm standard error from two independent experiments are shown. WT strain: N (number of cells) = 388; $\Delta cwsA$: N = 492.

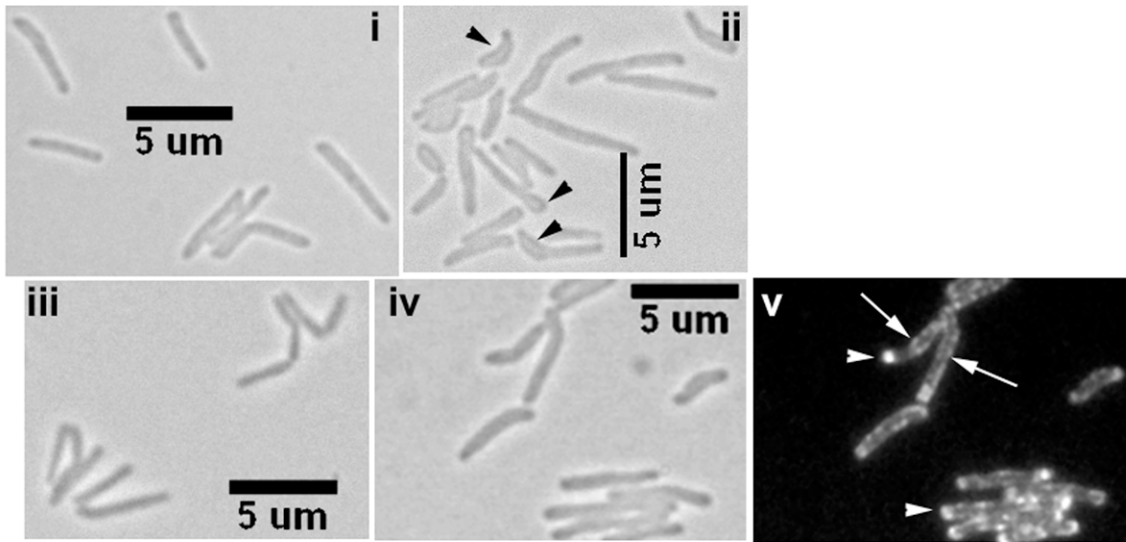


FIG. S4. Complementation of $\Delta cwsA$. Morphology of *M. smegmatis* wild-type (i), $\Delta cwsA$ (ii), $\Delta cwsA P_{cwsA}::cwsA$ (iii) and $\Delta cwsA P_{ami}::gfp-cwsA_{TB}$ (iv, v) was examined by microscopy. Panel v - fluorescent image corresponding to panel iv. Note reversal of $\Delta cwsA$ phenotype in complemented strains (iii and iv). Black arrowheads – bulged regions; white arrowhead – polar localization; white arrow – punctate localization.

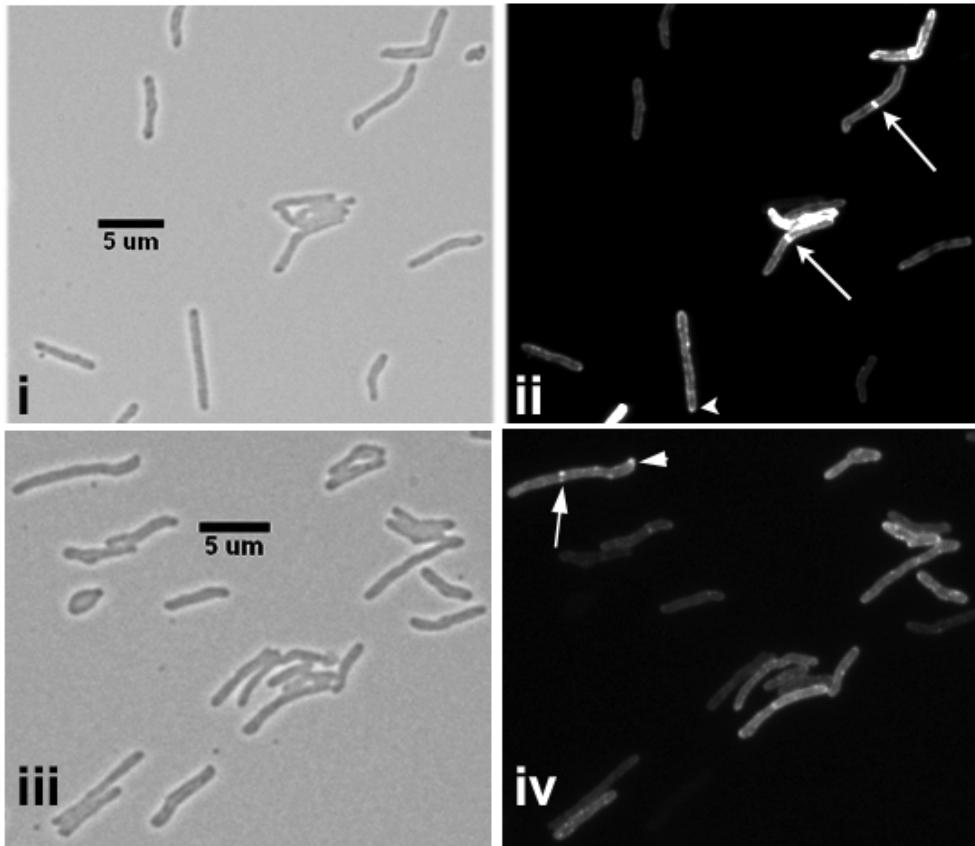


FIG. S5. ECFP-CrgA localization in $\Delta cwsA$. Actively growing cultures of *M. smegmatis* WT (i, ii) and $\Delta cwsA$ expressing *Pami::ecfp-crgA* (iii, iv) were imaged by brightfield (i, iii) and fluorescent (ii, iv) microscopy. Quantitation of CrgA localization from two independent experiments (N= 464) revealed a modest increase in ECFP-CrgA polar localization in $\Delta cwsA$ strain [$24.79 \pm 0.29\%$] as compared to wild type strain [$17.49 \pm 1.97\%$] but no significant difference in midcell localization [WT = $13.99 \pm 2.15\%$ vs $\Delta cwsA$ = $14.51 \pm 1.97\%$].

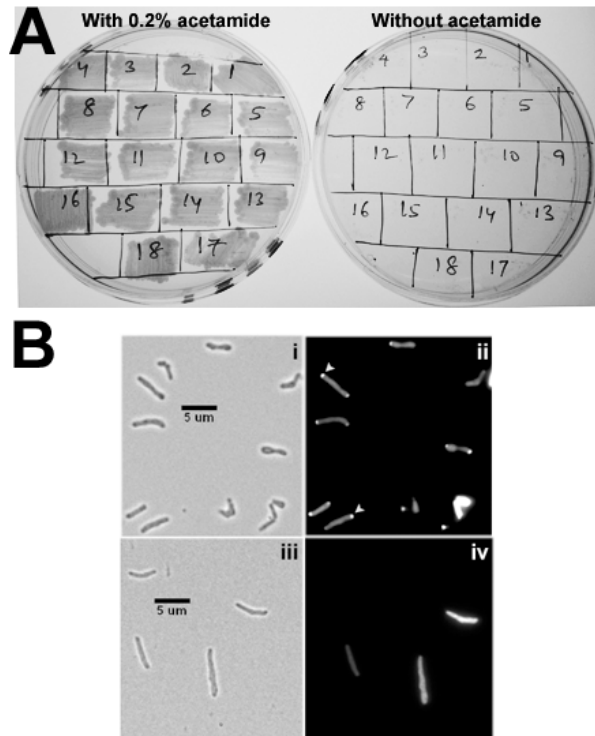


Fig. S6. Wag31-mCherry can complement $\Delta wag31$. (A) To establish the functionality of Wag31-mCherry, the integrated copy of *Pami::wag31* (Apramycin^R) in a *M. smegmatis* conditional mutant (Hyg^r) (Kang et al. 2008) was swapped with *Pami::wag31-mCherry* (Km^r resistant) as described (Chauhan et al. 2006) and transformants were selected on agar plates containing Hygromycin, Kanamycin and 0.2% acetamide. Colonies were patched on plates containing Hygromycin and kanamycin, but lacking acetamide. Note no growth was seen in the absence of acetamide (compare plates with and without acetamide). (B) Cells from + acetamide plate were propagated in broth containing appropriate antibiotics and 0.02% acetamide and examined by brightfield (i) and fluorescence (ii) microscopy. Arrowheads – polar localization of Wag31-mCherry. As control, *M. smegmatis* producing mCherry fluorescent protein was visualized by brightfield (iii) and fluorescence (iv) microscopy. Note diffuse localization with mCherry protein in panel iv.

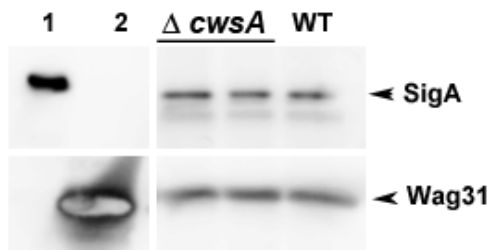


FIG. S7. Wag31 levels do not change in a $\Delta cwsA$ strain. Cell lysates prepared from *M. smegmatis* WT and $\Delta cwsA$ strain were separated in a SDS-PAGE gel, transferred to nitrocellulose membrane and analyzed by immunoblotting with α -Wag31 antibodies and α -SigA (loading control). Lane 1 – Purified His-SigA protein; lane 2 – purified His-Wag31 protein.

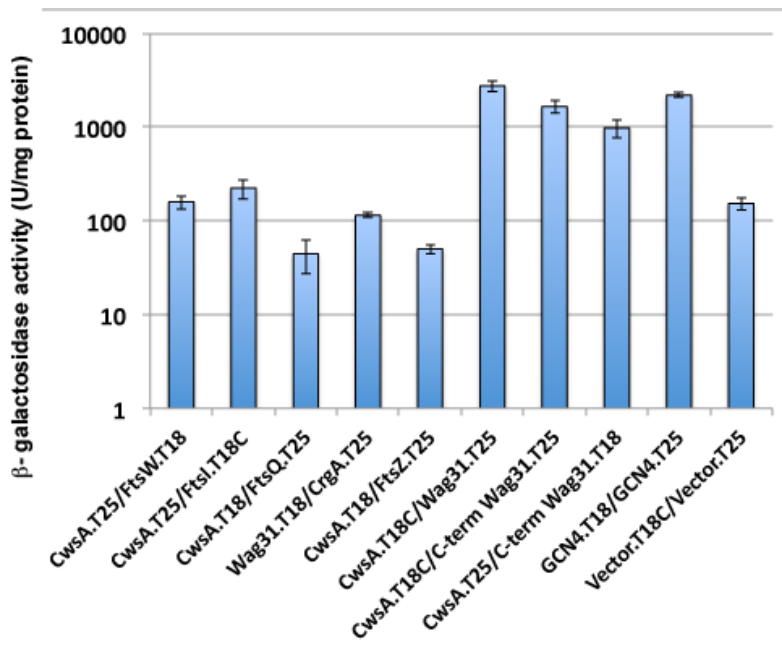


FIG. S8. BACTH assays. Indicated gene fusions to T25 and T18 fragments of adenylate cyclase in the BACTH vectors (Table 1) were used in various combinations to transform *E. coli* BTH101

and recombinants plated on LB agar supplemented with X-Gal and IPTG. Recombinant colonies were subsequently propagated in LB broth and β -galactosidase activity measured as described in the text. Values shown are means \pm standard deviations from at least 3 independent experiments.

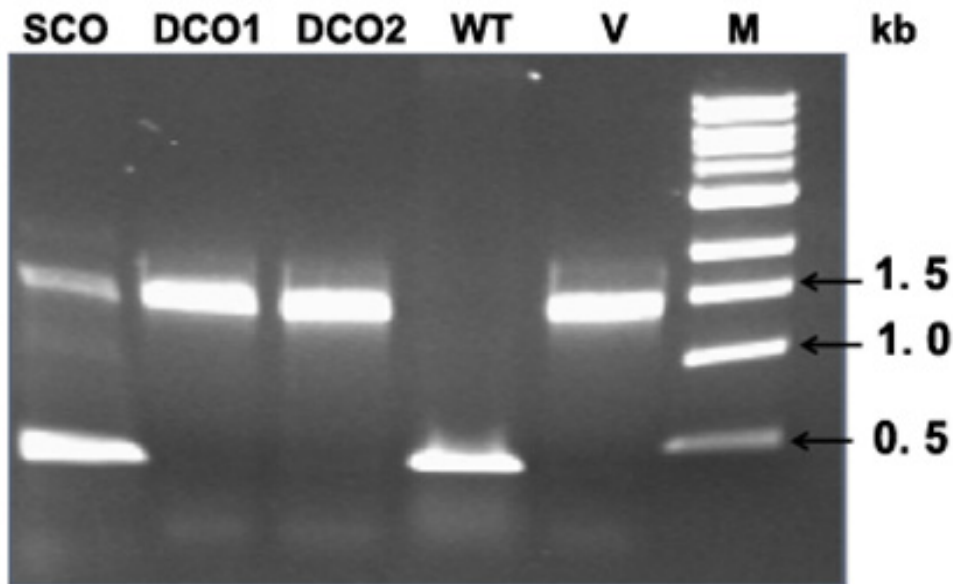


FIG. S9. Confirmation of DKO ($\Delta cwsA \Delta crgA$) strain by PCR. Genomic DNA from WT and DKO strains was used for PCR amplification of the *cwsA* region using primers *msmeg0023_F* and *msmeg0023_R* (Table S1). Amplified products were run on 1% agarose gels and photographed. Expected products are: WT = 411 – bp; single cross-over (SCO) = 411- and 1300 – bp; double cross-over = 1300 – bp and V = vector pPP116 (recombination plasmid for *cwsA* deletion; Table 1) = 1300 – bp.